

CRISPR/Cas9-mediated knockout of PIM3 suppresses tumorigenesis and cancer cell stemness in human hepatoblastoma cells

Raoud Marayati, M.D.^{1*}, Laura L. Stafman, M.D., Ph.D.^{1*}, Adele P. Williams, M.D.¹, Laura V. Bownes, M.D.¹, Colin H. Quinn, B.S.¹, Hooper R. Markert¹, Juliet L. Easlick, B.S.², Jerry E. Stewart, B.S.¹, David K. Crossman, Ph.D.³, Elizabeth Mroczek-Musulman, M.D.⁴, Elizabeth A. Beierle, M.D.¹

¹Division of Pediatric Surgery, Department of Surgery, University of Alabama at Birmingham, Birmingham, AL 35233, USA

²Division of Transplantation, Department of Surgery, University of Alabama at Birmingham, Birmingham, AL 35233, USA

³Department of Genetics, University of Alabama at Birmingham, Birmingham, AL 35233, USA

⁴Department of Pathology, The Children's Hospital of Alabama, Birmingham, AL 35233, USA

*These authors contributed equally to this work.

Running Title: PIM3 kinase promotes hepatoblastoma tumorigenesis and stemness

Corresponding Author

Elizabeth A. Beierle, MD

1600 7th Avenue South, Lowder Building, Suite 300

University of Alabama at Birmingham

Birmingham, AL 35233

Phone: (205) 638-9688, Fax: (205) 975-4972

e-mail: elizabeth.beierle@childrensal.org

The authors have no competing interests to disclose.

Supplementary Material

Figure S1

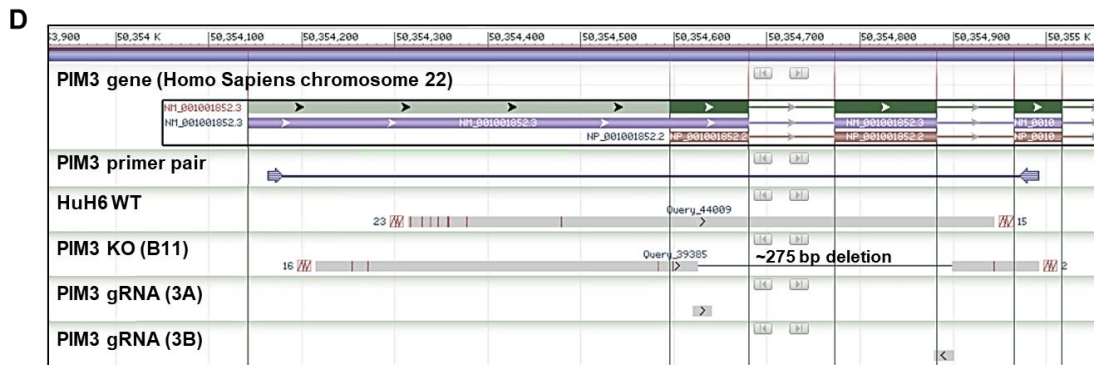
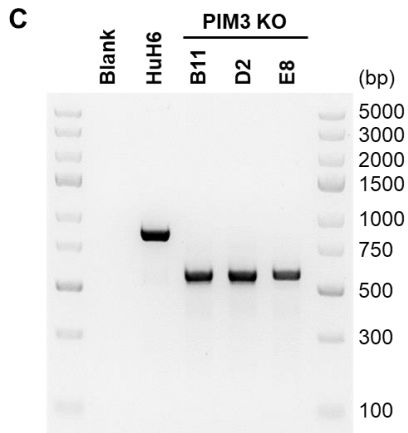
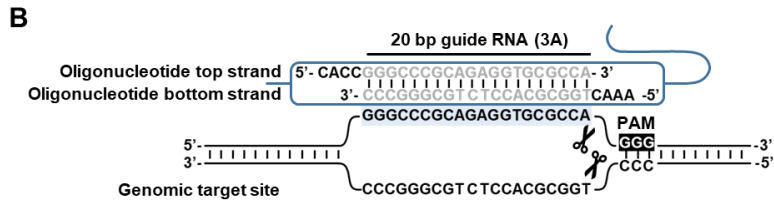
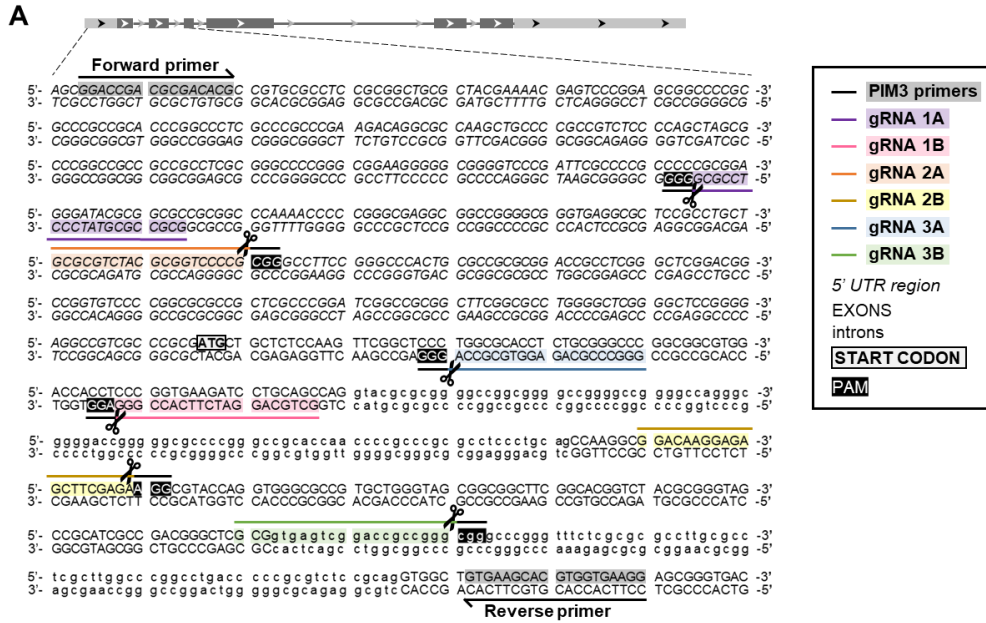


Figure S1. Establishment of stable CRISPR/Cas9-mediated PIM3 knockout cells. (A-B)

Design of PIM3 gRNAs and primers for knockout verification and sequencing. **(A)** Structure of the PIM3 gene is depicted at the top from 5' to 3' with exons indicated by dark grey boxes. Sequence for the region of interest (5' end of gene to 3' end of middle of exon 3) is listed underneath. The 5' untranslated region (UTR) is in italics, exons in uppercase, introns in lowercase, and PIM3 start codon in boxed bolded letters. gRNAs (*colored lines*) were designed to guide Cas9 to regions with PAM sequences (*black highlighted white text*). gRNAs were cloned into plasmids and cells were transfected with pairs of plasmids containing gRNA 1A and 1B, 2A and 2B, or 3A and 3B. The locations for the forward and reverse primers used in PCR to assess the edits are highlighted in grey. **(B)** Schematic diagram depicting the functionality of the CRISPR/Cas9 system. The sequences for the oligonucleotide top and bottom strand that were used to clone the gRNA 3A into the CRISPR/Cas9 plasmid are shown. Binding of the gRNA to the specific DNA target sequence preceding an adjacent PAM sequence “guides” the Cas9 enzyme to induce a double-strand break in the DNA target sequence. gRNA: Guide RNA; PAM: Protospacer adjacent motif. **(C)** PCR was performed on genomic DNA isolated from clones transfected with paired gRNAs. DNA was amplified using primers for the target region of PIM3 and gel electrophoresis was performed on PCR products. The unedited HuH6 band had an expected size of 828 bp. The 3 PIM3 knockout (KO) clones had smaller bands indicating large deletions. **(D)** Representative Sanger sequencing results of the HuH6 WT and PIM3 KO (clone B11) DNA. Following amplification with PIM3 primers (*pair shown as forward and reverse arrows*), PCR products were assessed using gel electrophoresis. Individual bands were cut out, DNA purified, and nucleotide sequence analyzed by Sanger sequencing. Results were aligned to the human reference sequence using BLAST. PIM3 KO had a large (~275 bp) deletion between the two gRNA cut sites. The gRNAs were also aligned and their position shown.

Figure S2

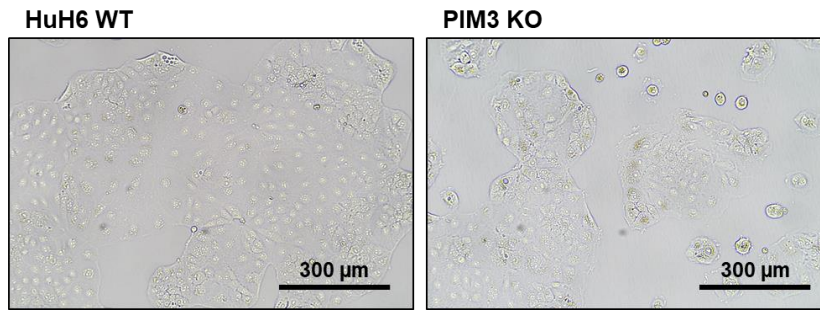


Figure S2. PIM3 knockout did not affect cell morphology. HuH6 WT or PIM3 KO cells (1×10^5) were plated into 6-well plates and imaged after 72 hours to assess for morphologic changes. The Photometrics CoolSNAP HQ2 CCD camera (Tucson, AZ) attached to a Nikon Eclipse Ti microscope (Tokyo, Japan) was used to image the plates and representative photomicrographs are shown. PIM3 KO cells did not differ in cell morphology from that of the HuH6 WT cell. Scale bars represent 300 μm.

Figure S3

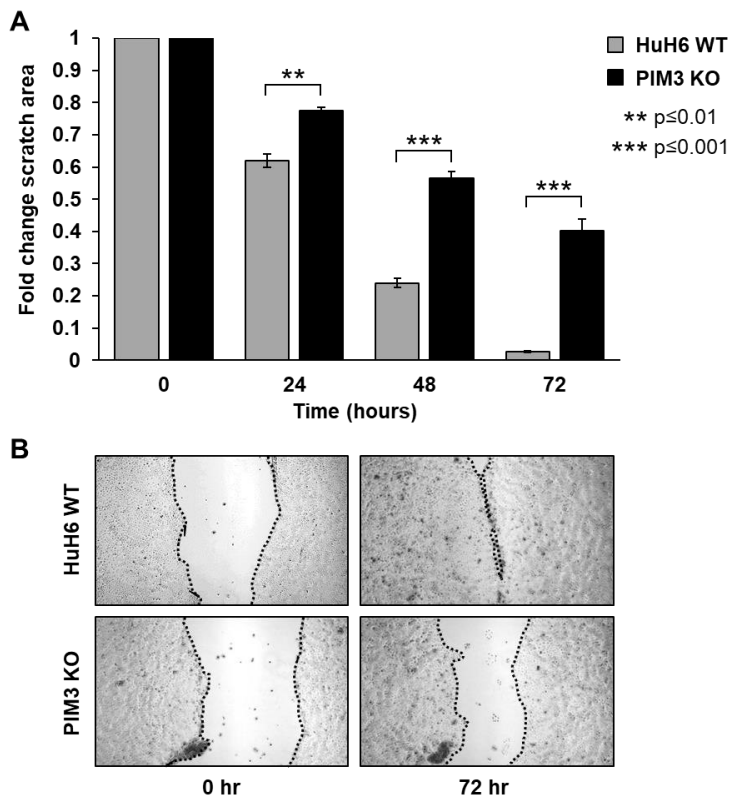


Figure S3. PIM3 knockout decreased motility in hepatoblastoma cells. Motility was evaluated utilizing a monolayer wounding (scratch) assay. HuH6 WT or PIM3 KO cells were plated and allowed to grow to near-confluency and a uniform scratch was made in the well. Images of the

scratch wound area were obtained at 0, 24, 48, and 72 hours. The area of the wound in pixels was quantified using ImageJ and data reported as mean fold change in scratch area compared to time zero \pm standard error of the mean. PIM3 KO cells resulted in significantly larger wound (scratch) area over time compared to HuH6 WT cells indicating decreased motility.

Figure S4

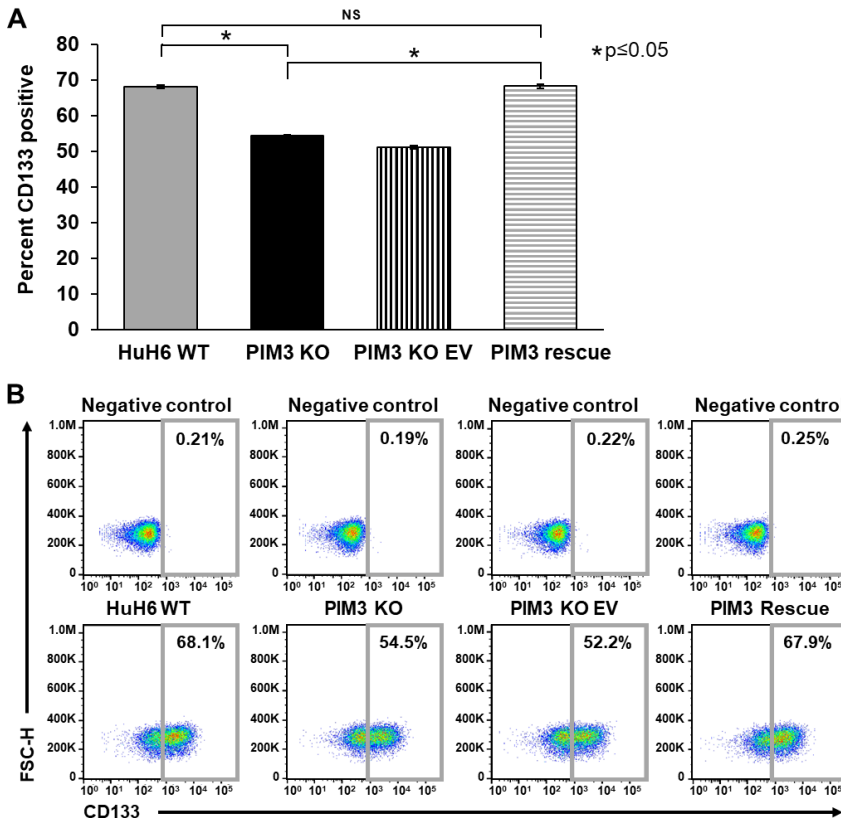


Figure S4. PIM3 re-introduction rescued the decrease in cancer cell stemness observed with PIM3 knockout. (A) Cell surface expression of CD133, a marker of hepatoblastoma stemness, was determined using flow cytometry in HuH6 wild-type (WT), PIM3 knockout (KO), or PIM3 KO cells transfected with either an empty vector (EV) control or PIM3 cDNA expressing plasmid (PIM3 Rescue). PIM3 KO led to significantly decreased CD133 expression compared to HuH6 WT cells, while re-introduction of PIM3 cDNA in PIM3 KO cells led to rescue of CD133 cell surface expression and a return to levels comparable to those seen in WT cells. There was no difference in CD133 expression between PIM3 rescue and HuH6 WT cells. Data represent at least three biologic replicates and are reported as mean \pm standard error of the mean. (B) Representative contour plots with negative staining controls for each cell line are shown. NS: non-significant.

Figure S5

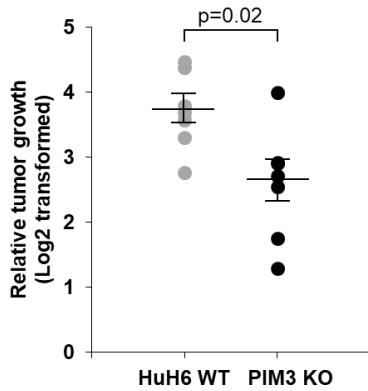


Figure S5. PIM3 knockout decreased *in vivo* tumor growth in male mice. HuH6 wild-type (WT) or PIM3 knockout (KO) cells were injected subcutaneously into the right flank of male athymic nude mice (n=7 per group) and tumor volume monitored over time. Male mice bearing PIM3 KO tumors exhibited a significantly decreased relative tumor growth compared to those bearing HuH6 WT tumors.

Figure S6

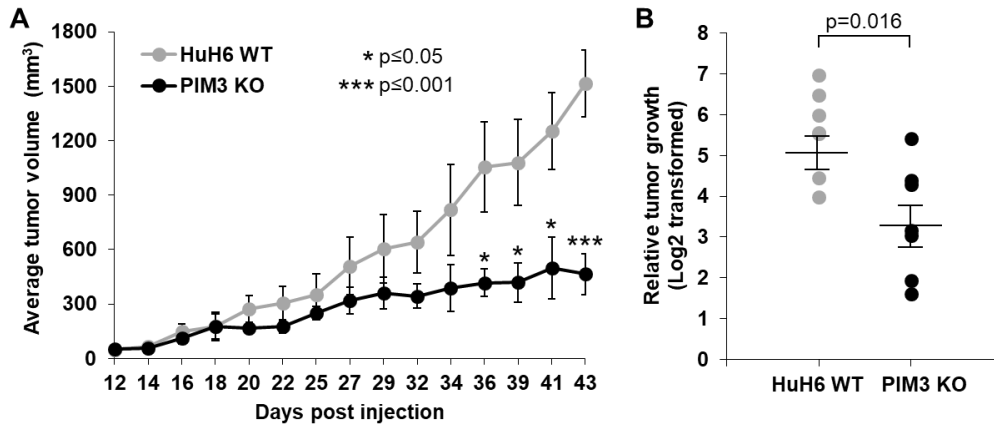


Figure S6. PIM3 knockout decreased *in vivo* tumor growth in female mice. (A) HuH6 WT and PIM3 KO cells were injected subcutaneously into the right flank and left flank, respectively, of 7 female athymic nude mice. PIM3 KO cells resulted in smaller tumors than those of HuH6 WT cells. (B) Relative tumor growth at the end of the 43-day study period was decreased in PIM3 KO tumors compared to WT tumors.

Table S1

gRNA	gRNA sequence	Oligonucleotide top strand sequence	Oligonucleotide bottom strand sequence
1A	GCGCCGCGTATCCCTCCGCG	CACCGCGCCGCGTATCCCTCCGCG	AAACGCGGAGGGATACGCGGCGC
1B	GCTGCAGGATCTTACCGGG	CACCGCTGCAGGATCTTACCGGG	AAACCCGGTGAAGATCCTGCAGC
2A	GCGCGTCTACGCGGTCCCG	CACCGCGGTCTACGCGGTCCCG	AAACCGGACCGCGGTAGACGCGC
2B	GGACAAGGAGAGCTTCGAGA	CACCGACAAGGAGAGAGCTTCGAGA	AAACTCTGAAGCTCTCCTTGTC
3A	GGCCCGCAGAGGTGCGCCA	CACCGGCCCGCAGAGGTGCGCCA	AAACTGGCGCACCTCTGCGGGCC
3B	CGGTGAGTCGGACCGCGGG	CACCGCGTGAGTCGGACCGCGGG	AAACCCGGCGGTCCGACTACCGC

Table S1: Table listing the gRNA sequences for CRISPR/Cas9-mediated editing of PIM3 gene and the oligonucleotide sequences used to clone gRNAs into CRISPR plasmid.

a specific disease or biological function is activated (positive z-score) or inactivated (negative z-score). The corresponding genes identified in the dataset are included.

Table S3

Ingenuity Canonical Pathway	p value	Ratio	z-score	Downregulated	Upregulated	Molecules
FXR/RXR Activation	4.07E-06	0.405	1.134	26/74 (35%)	48/74 (65%)	AHSG, ALB, AMBP, APOA1, APOA2, APOA4, APOC3, C3, CYP19A1, CYP27A1, FABP6, FBP1, FGA, FGF19, HPR, HPX, IL18, IL36G, IL37, KNG1, MAPK8, NR1H3, ORM1, ORM2, PLTP, RBP4, SLC27A5, SLC51A, TTR, VLDLR
Oxidative Phosphorylation	1.10E-04	0.365	4.811	8/74 (11%)	66/74 (89%)	ATP5F1B, ATP5F1C, ATP5F1D, ATP5MC1, ATP5ME, ATP5PF, COX4I1, COX4I2, COX5B, COX8B1, COX8C, COX7A2, COX7B, COX7B2, NDUFA1, NDUFA12, NDUFA3, NDUFAB1, NDUFB10, NDUFB11, NDUFB6, NDUFB7, NDUFB9, NDUFS3, NDUFS7, NDUFV1, UQCRC1
LXR/RXR Activation	1.29E-04	0.373	3.128	20/67 (30%)	47/67 (70%)	AHSG, ALB, AMBP, APOA1, APOA2, APOA4, APOC3, C3, ECHS1, FGA, HPR, HPX, IL18, IL36G, IL37, KNG1, LBP, NCOR1, NR1H3, ORM1, ORM2, PLTP, RBP4, TNFRSF1B, TTR
Histidine Degradation VI	1.70E-03	0.667	1.633	2/9 (22%)	7/9 (78%)	AMDHD1, CYP26B1, CYP2E1, CYP4F11, CYP7B1, UROC1
CCR5 Signaling	3.63E-03	0.356	-2.828	30/45 (67%)	15/45 (33%)	CACNA1D, CACNA1H, CACNG4, CAMK4, CD3D, CD3G, FAS, FCER1G, GNAI1, GNG4, JUN, MAPK1, MAPK8, PRKCE, PRKCI, PRKCB
Pregnenolone Biosynthesis	6.31E-03	0.625	1	2/8 (25%)	6/8 (75%)	CYP26B1, CYP27A1, CYP2E1, CYP4F11, CYP7B1
LPS/IL-1 Mediated Inhibition of RXR Function	9.33E-03	0.266	-1	56/128 (44%)	72/128 (56%)	ABCB1, ABCG3, ACSBG1, ALDH3A1, CHST10, CHST2, CHST3, CPT1A, CPT1C, FABP1, FABP5, FABP6, FMO1, FMO5, GSTA1, HMGCS2, HS3ST5, IL18, IL36G, IL37, JUN, LBP, MAOB, MAPK8, MGMT, MGST3, NDST1, NR1H3, PLTP, SLC27A5, SULT1C2, SULT1C4, TNFRSF1B, UST
VDR/RXR Activation	1.45E-02	0.319	1.265	25/47 (53%)	22/47 (47%)	CALB1, CST6, EP300, HSD17B2, IGFBP6, KLF4, KLF6, NCOA3, NCOR1, PRKCE, PRKCI, PRKCB, SPP1, TGFβ2, VDR
Melatonin Signaling	1.45E-02	0.319	-1.291	30/47 (64%)	17/47 (36%)	CAMK4, GNAI1, GNRH1, GNRH2, MAP2K2, MAP2K6, MAPK1, NOTUM, PLCD3, PLCE1, PRKACB, PRKCE, PRKCI, PRKCB, RORA
Osteoarthritis Pathway	1.66E-02	0.256	-1.061	78/133 (59%)	55/133 (41%)	ACVRL1, ADAMTS4, ALPI, ALPL, BMP1R1A, CASP5, CASP8, CASP9, CTNBB1, DDR2, DLX5, EPAS1, FGF18, FGF2, FGF8, FGF9, FRZB, FZD3, FZD6, ITGB1, JAG1, LEF1, MATN3, MMP1, PRKAA1, PRKAA2, RARRS2, RBP4, SIRT1, SMAD1, SMAD5, SPP1, TCF4, TNFRSF1B
GPCR-Mediated Nutrient Sensing in Enteroendocrine Cells	2.00E-02	0.302	-1	34/53 (64%)	19/53 (36%)	ADCY1, CACNA1D, CACNA1H, CACNG4, GAST, GNAI1, GNG4, ITPR2, NOTUM, PLCD3, PLCE1, PRKACB, PRKCE, PRKCI, PRKCB, TRPM5
Nitric Oxide Signaling in the Cardiovascular System	2.00E-02	0.302	-2	35/53 (66%)	18/53 (34%)	CACNA1D, CAMK4, GUCY2C, ITPR2, KNG1, MAP2K2, MAPK1, PDE1C, PDE3B, PDE5A, PIK3CA, PRKAA1, PRKACB, PRKCE, PRKCI, PRKCB
Bile Acid Biosynthesis, Neutral Pathway	2.29E-02	0.571	1	4/7 (57%)	3/7 (43%)	AKR1C1/AKR1C2, CYP27A1, HSD3B7, SLC27A5
Nicotine Degradation II	2.34E-02	0.381	2.121	6/21 (29%)	15/21 (71%)	AOX1, CYP19A1, CYP2E1, CYP2F1, FMO1, FMO5, UGT1A1, UGT2A1
Sperm Motility	2.34E-02	0.254	-2.496	75/122 (61%)	47/122 (39%)	AATK, AXL, CACNA1H, CAMK4, CNGA1, CSF1R, DDR2, EPHA2, EPHA4, EPHB4, FGF3, ITPR2, JAK2, LCK, LMTK2, LYN, MAP2K6, NOTUM, NPPC, PDE1C, PLCD3, PLCE1, PRKACB, PRKCE, PRKCI, PRKCB, PTK2, SLC12A2, SLC16A10, SRMS, TWIF1
CDK5 Signaling	3.09E-02	0.189	-2	49/74 (66%)	25/74 (34%)	ADCY1, BDNF, GNAI1, ITGB1, MAP2K2, MAPK1, MAPK8, PPP1R12A, PPP1R14A, PPP1R14B, PPP1R3D, PPP2R2C, PRKACB, RASD1
Leptin Signaling in Obesity	3.16E-02	0.298	-1.414	35/47 (74%)	12/47 (26%)	ADCY1, AGRP, GHR1, JAK2, LEPR, MAP2K2, MAPK1, NOTUM, PDE3B, PIK3CA, PLCD3, PLCE1, PRKACB, SOCS3
BMP signaling pathway	3.63E-02	0.279	-3.207	42/61 (69%)	19/61 (31%)	BMP4, BMP8A, BMP1R1A, CAMK4, JUN, MAGED1, MAP2K2, MAPK1, MAPK8, NKX2-5, PRKACB, RASD1, SMAD1, SMAD5, SOST, TAB1, ZNF423
eNOS Signaling	3.72E-02	0.262	-1.698	47/84 (56%)	37/84 (44%)	ADCY1, AQP10, CAMK4, CASP8, CASP9, CHRM5, CHRNA9, CHRNE, CNGA1, ESR1, HSPA1A/HSPA1B, ITPR2, KNG1, LPAR1, NOS1P, PIK3CA, PRKAA1, PRKAA2, PRKACB, PRKCE, PRKCI, PRKCB
Calcium Signaling	3.80E-02	0.252	-1.5	59/103 (57%)	44/103 (43%)	ACTA2, ACTC1, ATP2B1, CACNA1D, CACNA1H, CACNG4, CALR, CAMK4, CHRNA9, CHRNE, EP300, GRIN1, HDAC11, ITPR2, MAPK1, MEF2A, MYH14, MYH9, MYL2, MYL4, PNCK, PRKACB, SLC8A2, TNCC2, TRPC1, TRPM8
Cell Cycle: G1/S Checkpoint Regulation	4.07E-02	0.14	-1.604	35/56 (63%)	21/56 (38%)	CDKN2C, HDAC11, RB1, TGFβ2
NF-κB Signaling	4.17E-02	0.214	-1.663	75/117 (64%)	42/117 (36%)	BMP4, BMP1R1A, CASP8, CSNK2B, EGF, EP300, FCER1G, FGF3, IL18, IL36G, IL37, LCK, MAP2K6, MAPK8, NFKBID, PIK3CA, PRKACB, PRKCB, RASD1, TAB1, TNFAIP3, TNFRSF11A, TNFRSF1B, TNFSF13B, TRAF5
Synaptogenesis Signaling Pathway	4.17E-02	0.231	-2.214	111/186 (60%)	75/186 (40%)	ADCY1, AP2S1, BAD, BDNF, CAMK4, CDH16, CDH3, CDH6, CHN1, CPLX1, CRK, CTNBB1, EFNB1, EFNB3, EIF4EBP1, EPHA10, EPHA2, EPHA4, EPHB4, GRIN1, LCK, LYN, MAP1B, MAPK1, NHP1L4, PIK3CA, PRKACB, PRKCE, RAPGEF1, RASD1, SGTA, SHC3, SNGO, SOST, STXBP1, STXBP4, STXBP5, SYT12, SYT5, THBS1, TIAM1, VLDLR, WAS
PI3K/AKT Signaling	4.79E-02	0.312	-1.897	18/32 (56%)	14/32 (44%)	CASP9, CRK, GNAI1, KPNA3, MAP2K2, MAPK1, NFKBID, PIK3CA, PLAC8, ZNF346
Corticotropin Releasing Hormone (CRH) Signaling	4.90E-02	0.26	-2	53/77 (69%)	24/77 (31%)	ADCY1, BDNF, CACNA1D, CACNA1H, CACNG4, CAMK4, GAD1, GAST, GNAI1, GUCY2C, ITPR2, JUN, MAP2K2, MAPK1, MEF2A, NR4A1, PRKACB, PRKCE, PRKCI, PRKCB
TGF-β Signaling	4.90E-02	0.26	-2.5	57/77 (74%)	20/77 (26%)	ACVR1B, BMP4, BMP1R1A, EP300, JUN, MAP2K2, MAP2K6, MAPK1, MAPK8, NKX2-5, RASD1, SERPINE1, SKI, SMAD1, SMAD5, SOST, TAB1, TGFβ2, VDR, ZNF423
mTOR Signaling	5.01E-02	0.14	-2.309	65/150 (43%)	85/150 (57%)	EIF3C, EIF3G, EIF3J, EIF4EBP1, MAPK1, PIK3CA, PLD4, PPP2R2C, PRKAA1, PRKAA2, PRKCE, PRKCI, PRKCB, RAC2, RASD1, RHOQ, RPS15, RPS28, RPS29, RPS9, ULK1

Table S3: Table containing the top canonical pathways identified by IPA to be significantly activated (z-score>+1) or inactivated (z-score<-1) for the differentially regulated genes following PIM3 KO (p<0.05 and fold change cutoff ± 2). The ratio indicates the number of genes from the dataset that map to the pathway divided by the total number of proteins that map to the same pathway. Genes in the dataset that are involved in each canonical pathway are included and are broken down as downregulated and upregulated. Representative percentages of present versus total genes per canonical pathway are shown between parentheses.